RSC Advances

PAPER

View Article Online
View Journal | View Issue

Check for updates

Cite this: *RSC Adv.*, 2020, **10**, 10471

Characterization of bitumen and a novel multiple synergistic method for reducing bitumen viscosity with nanoparticles and surfactants

Yunfeng Liu,[a] Zhengsong Qiu,*[a] Chong Zhao,[a] Zhen Nie,[b] Hanyi Zhong,[a] Xin Zhao,[a] Shujie Liu[c] and Xijin Xing[c]

Received 12th January 2020
Accepted 6th March 2020

DOI: 10.1039/d0ra00335b

rsc.li/rsc-advances

This paper is concerned with the formation of bitumen during the drilling of the H oilfield in Iraq. The high viscosity and strong adhesion properties of bitumen can influence the drilling operations. Some complex problems include paste screening, and drill pipe sticking, which cause huge economic losses. Therefore, it is necessary to effectively reduce the bitumen viscosity. The contribution of a single subcomponent of bitumen to the viscosity can vary, and the combined effect of different components of bitumen on the viscosity remains unclear. Furthermore, the mechanism of viscosity reduction remains unclear. In this study, the effects of organic solvents on the viscosity of bitumen were studied, and toluene was selected as the best organic solvent. The results showed that aromatics/resins, aromatics/asphaltenes, and resin/asphaltenes can help increase the bitumen viscosity. Novel methods, including the use of nanoparticles, ethyl cellulose, and the quaternary ammonium salt of heptadecenyl hydroxyethyl imidazoline (QASHI), were proposed to decrease the viscosity. TiO_2 and CuO nanoparticles were chosen, and the main factors influencing the viscosity, such as the particle type, concentration, particle size, temperature, and shear rate, were analysed. The results show that the bitumen viscosity decreases with the increase in the concentrations of ethyl cellulose and QASHI. A synergistic effect between ethyl cellulose and QASHI was found with an optimal concentrations of ethyl cellulose and QASHI (1000 and 1600 mg L^{-1}). A synergistic effect was also observed when nanoparticles, ethyl cellulose, and QASHI were used in combination. This paper reports the micro-mechanism whereby the viscosity of bitumen is decreased.

Open Access Article. Published on 11 March 2020. Downloaded on 12/26/2025 7:02:38 PM.
This article is licensed under a Creative Commons Attribution-NonCommercial 3.0 Unported Licence.

1. Introduction

During the drilling of the H oilfield in Iraq, highly viscous bitumen was encountered. With plastic creep characteristics and strong cohesion [1–4], bitumen deteriorates the properties of the drilling fluid and increases the risk of drill pipe sticking.[5,6] This could reduce the rate of penetration (ROP) and extend the non-productive time (NPT), causing significant economic losses. Fig. 1 shows the bitumen circulated back with the drilling fluid in the drilling field.

The macroscopic phenomenon is controlled by microscopic mechanisms. To understand the high viscosity of bitumen, it is important to analyse the basic chemical components and their effect on viscosity. A saturate, aromatic, resin, and asphaltene (SARA) analysis has shown that the bitumen formed mainly includes saturates, aromatics, resins, and asphaltenes.[5–7] Different subfractions have shown different density and viscoelasticity.[5,8,9] Early studies[10] have found that increasing the content of asphaltene can increase the viscosity of bitumen. Asphaltene has a high percentage of heteroatoms (N, O, S, and metals), and its self-aggregation effect will further increase the structural complexity of bitumen.[11–13] However, studies on the influence of other components on the viscosity of bitumen, including saturates, aromatics, and resins, are lacking. In addition, the relationship between the different subfractions in increasing the bitumen viscosity is unclear.

The most straightforward method of solving the bitumen formation problem is reducing its viscosity.[14–18] Many researchers have designed novel viscosity reducers to decrease the viscosity, with good effect.[17,19–25] However, the synthesis methods are complex and difficult to be applied to industrial production. Nik *et al.* prepared oxidised asphaltene as a viscosity reducer for bitumen. Although the viscosity reduction effect is good, the preparation process is complicated and unsuitable for large-scale industrial applications. Mortazavi-Manesh and Shaw prepared a novel copolymer as a bitumen viscosity reducer; however, it is difficult to apply this method to industrial applications. Recently, nanoparticles have been widely used in the petroleum industry for applications such as enhanced oil recovery (EOR),[26–28] emulsion stability and demulsification,[29] and heat conducting processes.[30,31] The

[a]School of Petroleum Engineering, China University of Petroleum (East China), 266580 Qingdao, China. E-mail: b15020047@s.upc.edu.cn
[b]China National Petroleum Corporation (CNPC) Research Institute of Petroleum Exploration and Development, 100083 Beijing, China
[c]CNOOC Research Institute Co. Ltd., 100028 Beijing, China

Open Access Article. Published on 11 March 2020. Downloaded on 12/26/2025 7:02:38 PM.
This article is licensed under a Creative Commons Attribution-NonCommercial 3.0 Unported Licence.

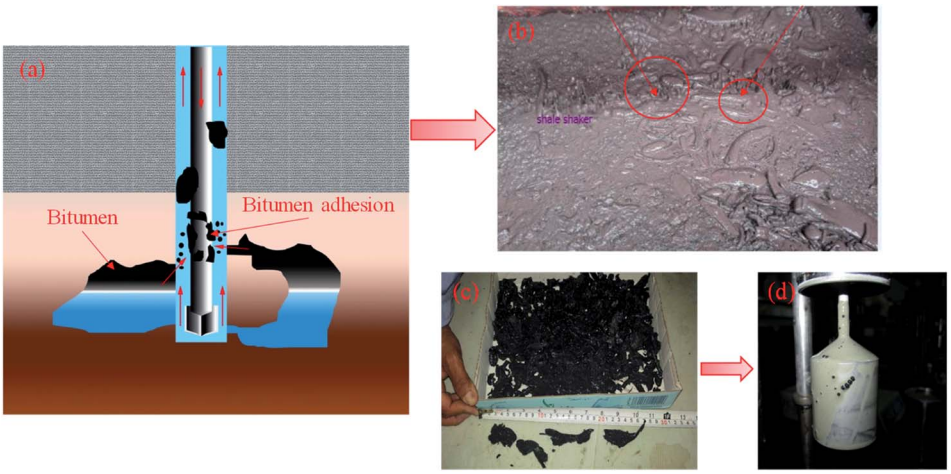

Fig. 1 Bitumen encountered during the drilling of the H oilfield: (a) schematic of bitumen formation in the drilling process; (b) different scales of bitumen mixtures in drilling fluid; (c) bitumen collected from the drilling fluid; (d) rheological property test of drilling fluid contaminated with bitumen pollution (bitumen easily adhere and stuck the drill pipe).

Table 1 Various chemical additives used in the experiments and their corresponding manufacturers

Chemical additives	Manufacturers	Purity
TiO_2 nanoparticles (with diameters of 10, 20, 50, and 100 nm)	Aladdin Chemistry Co. Ltd.	≥99%, analytical purity
CuO nanoparticles (with diameters of 10, 20, 50, and 100 nm)		≥99%, analytical purity
Al_2O_3		30 nm, analytical purity
Toluene, *n*-heptane, methanol, *p*-xylene, cyclopentane, trichloroethylene, ethanol, chloroform, QASHI, *et al.*	Qingdao Macklin Biochemical Co., Ltd	Chemically purity

viscosity of bitumen is mainly associated with the formation of a viscoelastic network between asphaltene nanoaggregates or asphaltene and other bitumen subfractions. Nanoparticles have a strong adsorption affinity with asphaltenes and are expected to help decrease bitumen viscosity owing to their small size, high surface area-to-volume ratio, dispersibility, and high adsorption affinity. However, nanoparticles have rarely been employed in this field.

In this study, the contributions of the basic components of bitumen to its viscosity were analysed. Nanoparticles were innovatively introduced to reduce the viscosity with surfactants, and a systematic optimisation of viscosity decreasing additives formula is provided. Ethyl cellulose and QASHI were chosen to decrease the viscosity. The synergistic micro-mechanism between ethyl cellulose (QASHI surfactant) and the nanoparticles in reducing the bitumen viscosity was revealed. This is a fundamental study for the development of a novel anti-bitumen drilling fluid formula.

2. Materials and methods

2.1 Materials

Various chemical reagents were used in the experiments. Table 1 lists the names of the chemical additives and of their manufacturers.

Bitumen samples (85.6% content) were obtained from the Mishrif Formation in the H oilfield, Iraq. The depth of this stratum is in the range of approximately 3200–4500 m, thus falling in the limestone stratum range. Bitumen is formed at many locations in this layer, and its distribution is irregular. 20 of different depth bitumen samples were took, and then the samples were mixed, and the bitumen were extracted from the mixed samples. Table 2 lists the detailed properties of bitumen.

2.2 Methods

Fig. 2 shows a flowchart of the research conducted in this study.

Table 2 Elemental and SARA analyses, including the density and viscosity of bitumen

Elemental analysis (wt%)	C	H	O	N	S
	83.4	9.6	0.1	0.5	6.4
SARA analysis (wt%)	**Saturate**	**Aromatic**	**Resin**	**Asphaltene**	
	34.7	26.8	19	19.5	
Density (g /cm^{-3}3)	1.2	Viscosity (mPa ·s)	128 000	Softening point (°C)	117.9

This journal is © The Royal Society of Chemistry 2020

Open Access Article. Published on 11 March 2020. Downloaded on 12/26/2025 7:02:38 PM.
This article is licensed under a Creative Commons Attribution-NonCommercial 3.0 Unported Licence.

2.2.1 Bitumen extraction and SARA analysis. Fig. 3 shows the detailed experimental procedures for bitumen recovery and SARA analysis. The experimental procedure was in accordance with those in previous studies,[32,33] and the (SARA) fractionation of bitumen was performed as per ASTMD4124.[5]

First, 10 g of the crude bitumen sample was mixed in 60 mL of toluene. Ultrasound extraction was carried out for 1 h. The soluble components were sent to a rotary evaporator; the insoluble components were solids. After toluene extraction, 7.62 g of bitumen was extracted from the crude bitumen samples. This bitumen was used for the viscosity reduction experiment.

Second, 3 g of bitumen was poured into a 500 mL beaker, and 200 mL of *n*-heptane was added. A sonicated extraction was conducted at 50 °C for 30 min. The insoluble and soluble components were separated through centrifugation conducted at 8000 rpm for 10 min. The insoluble solids were asphaltenes, and the soluble components were saturate, aromatic, and resin (SAR) components. Thereafter, the soluble components were filtered, and the SAR components were then loaded onto the Al_2O_3 column. The SAR components were collected individually by elution with 100 mL of heptane and 100 mL of mixed organic solvent (methanol/toluene (V/V, 1 : 1)).

2.2.2 Viscosity measurements. The viscosity was measured using the MCR 301 rheometer (Anton Paar Germany GmbH, Graz, Austria). The rheological measurements were conducted in a temperature range of 20–60 °C and a shear rate range of 0–80 s^{-1}. Every experiment was repeated at least three times; the final value was the average of the three.

(1) Role of organic solvents in decreasing bitumen viscosity. Organic solvents, including toluene, *p*-xylene, and cyclopentane, were used to decrease the viscosity of bitumen. One gram of bitumen was diluted in different amounts (0–1 mL) of organic solvents. The viscosity was measured at 20 °C and at a shear rate of 20 s^{-1}.

(2) Effects of bitumen components on viscosities of SARA-toluene solutions. To study the role of saturate, aromatic, resin, and asphaltene components in decreasing the bitumen viscosity,

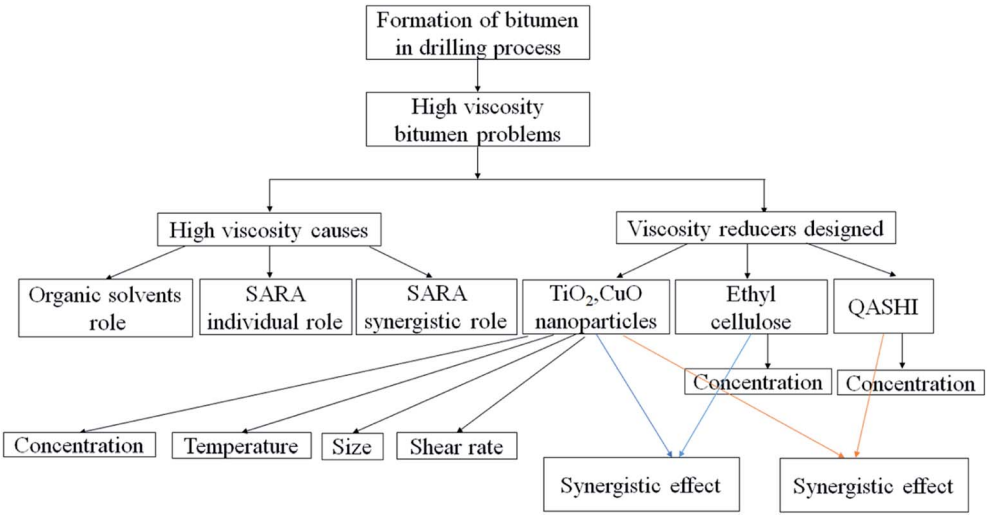

Fig. 2 Flowchart of the research procedure.

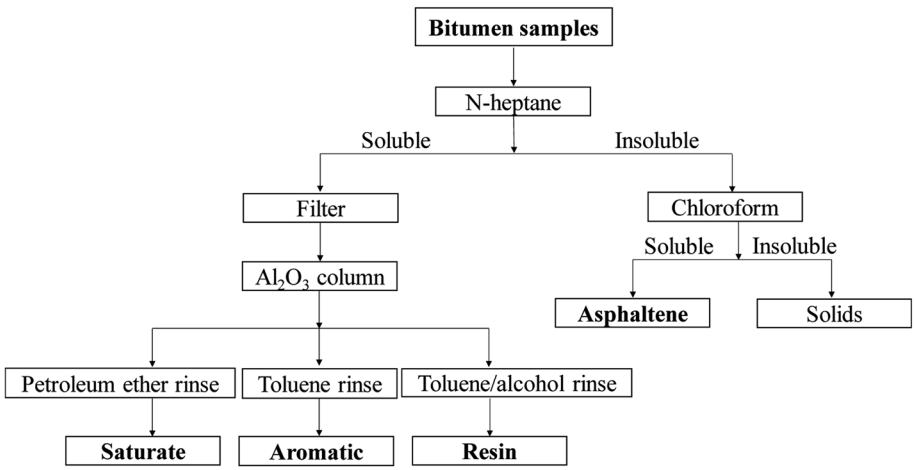

Fig. 3 Experimental procedure of bitumen extraction and separation of saturate, aromatic, resin, and asphaltene components from bitumen.

Open Access Article. Published on 11 March 2020. Downloaded on 12/26/2025 7:02:38 PM.
This article is licensed under a Creative Commons Attribution-NonCommercial 3.0 Unported Licence.

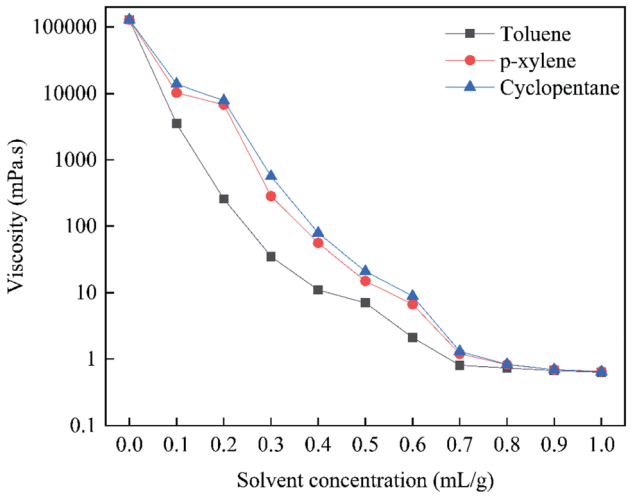

Fig. 4 Viscosities of bitumen diluted with different concentrations of organic solvents at 20 °C and at a shear rate of 20 s^{-1}.

the viscosity measurements of the saturate, aromatic, resin, and asphaltene-toluene solutions were repeated by preparing samples with different mass concentrations (0, 0.1, 0.2, 0.3, 0.4, and 0.5 g mL^{-1}) at 20 °C and at a shear rate of 20 s^{-1}. Moreover, the synergistic effect between the components was studied. The saturate/aromatic, saturate/resin, saturate/asphaltene, aromatic/resin, aromatic/asphaltene, and resin/asphaltene mixtures were used to prepare the mixture-toluene solutions at different concentrations. The viscosities were measured at 20 °C and at a shear rate of 20 s^{-1}.

(3) Effect of temperature on viscosities of 0.5 g mL^{-1} SARA-toluene solutions. The viscosity measurements of the saturate, aromatic, resin, and asphaltene-toluene solutions were repeated for a 0.5 g mL^{-1} sample in the temperature range of 20–60 °C and at a shear rate of 20 s^{-1}.

(4) Effects of temperature and nanoparticle concentration on bitumen viscosity. To study the role of nanoparticles in decreasing the bitumen viscosity, the nanoparticles were mixed with bitumen at a stirring rate of 300 rpm for 1 h. The nanoparticles dispersed into the bitumen uniformly. In this study, 20 nm TiO_2 and 20 nm CuO were selected as the nanoparticles. The effect of different nanoparticle concentrations (0, 100, 500, 1000, 2500, 5000, and 10 000 mg L^{-1}) on the viscosity of bitumen at different temperatures (20, 30, 40, 50, and 60 °C) and at a shear rate of 20 s^{-1} was studied.

(5) Effects of nanoparticle size and shear rate on bitumen viscosity. Because different nanoparticle sizes can influence the surface area, the nanoparticle size could influence the bitumen viscosity. In this study, 2500 mg L^{-1} of TiO_2 and 1000 mg L^{-1} of CuO were chosen, because at this concentration, the nanoparticles showed the highest viscosity reduction effect. To study

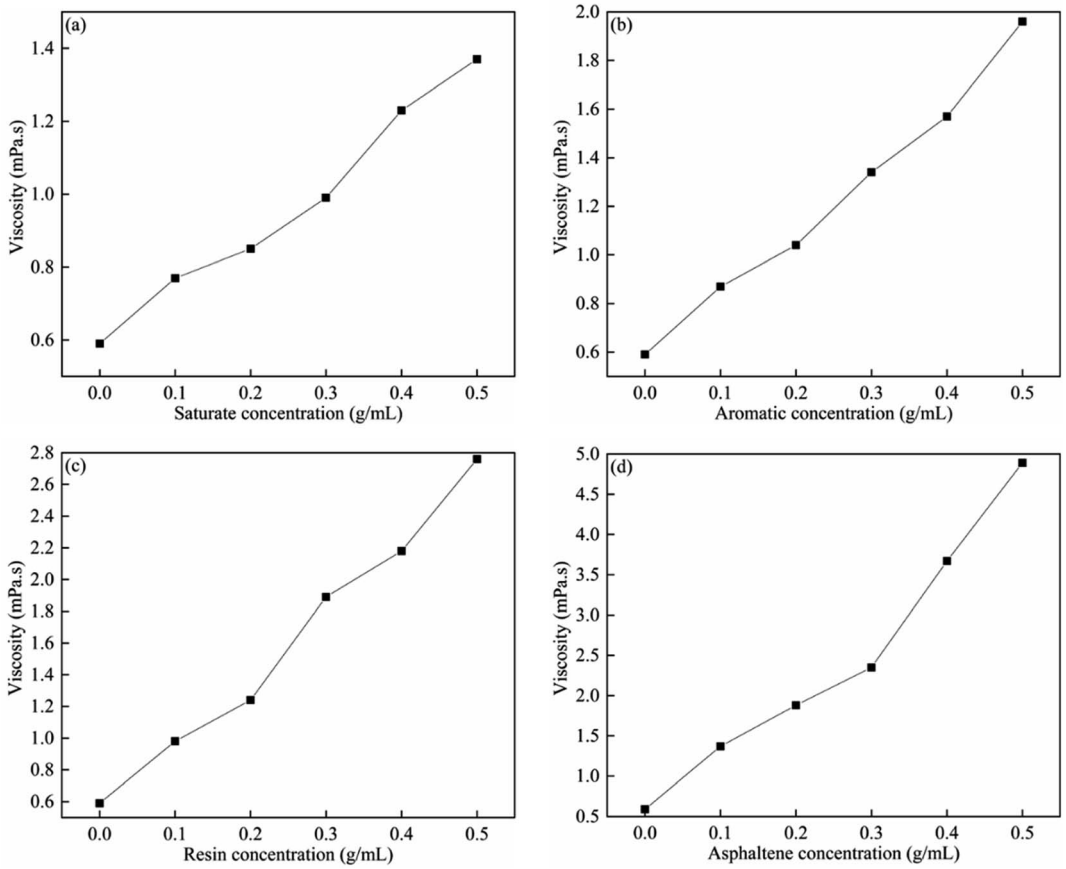

Fig. 5 Viscosities of (a) saturate; (b) aromatic; (c) resin; (d) asphaltene-toluene solutions with different concentrations at 20 °C and at a shear rate of 20 s^{-1}.

 This journal is © The Royal Society of Chemistry 2020

Open Access Article. Published on 11 March 2020. Downloaded on 12/26/2025 7:02:38 PM.
This article is licensed under a Creative Commons Attribution-NonCommercial 3.0 Unported Licence.

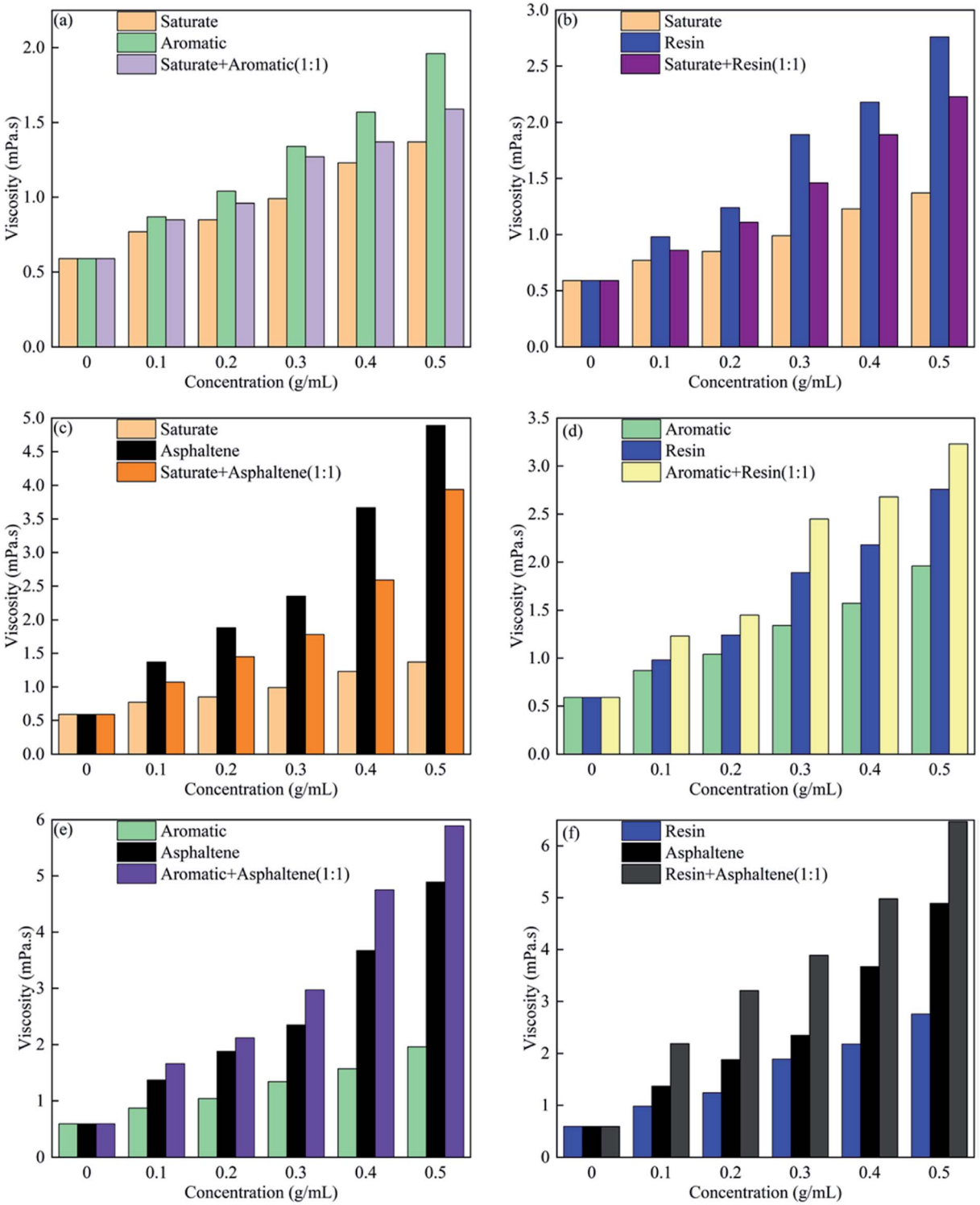

Fig. 6 Viscosities of (a) saturate, aromatic; (b) saturate, resin; (c) saturate, asphaltene; (d) aromatic, resin; (e) aromatic, asphaltene; (f) resin, asphaltene-toluene solutions with different concentrations at 20 °C and at a shear rate of 20 s^{-1}.

the nanoparticle size effect on the bitumen viscosity, 10, 20, 50, and 100 nm TiO_2 and CuO nanoparticles were used. Because bitumen is a non-Newtonian fluid, and the viscosity is not linear with the shear rate, the variation in the bitumen viscosity at different shear rates (20, 40, 60, and 80 s^{-1}) was studied.

(6) Effects of ethyl cellulose and QASHI concentration on bitumen viscosity. Ethyl cellulose has been widely used for decreasing the viscosity of emulsions.[34–36] However, reports on the use of ethyl cellulose for decreasing bitumen viscosity are limited, but many researches focused on the ethyl cellulose help bitumen recovery.[37,38] In this study, ethyl cellulose and QASHI

Open Access Article. Published on 11 March 2020. Downloaded on 12/26/2025 7:02:38 PM. This article is licensed under a Creative Commons Attribution-NonCommercial 3.0 Unported Licence.

were added to bitumen with different concentrations and stirred at 300 rpm for 1 h. The viscosity was measured at 20 °C and at a shear rate of 20 s^{-1}. The concentrations of ethyl cellulose and QASHI were in the range of 0–2000 mg L^{-1}.

(7) Synergistic effect of ethyl cellulose (QASHI) and nanoparticles on decreasing bitumen viscosity. The nanoparticles and ethyl cellulose (QASHI) were mixed in bitumen at optimal concentrations. The stirring rate was 300 rpm, and the stirring time was 1 h. The bitumen viscosity was measured at 20 °C and at a shear rate of 20 s^{-1}.

3. Results and discussion

3.1 Effect of organic solvent on decreasing bitumen viscosity

Fig. 4 shows the viscosities of bitumen diluted with different organic solvents at 20 °C and at a shear rate of 20 s^{-1}. Toluene, *p*-xylene, and cyclopentane help decrease the bitumen viscosity. When the organic concentration is lower than 0.3 mg L^{-1}, the viscosity reducing capacity is as follows: toluene > *p*-xylene > cyclopentane. This is because toluene and *p*-xylene are aromatic solvents and have better solubility with the aromatic, resin, and asphaltene components in bitumen.[39,40] When the organic solvent concentration is 0.1 mg L^{-1}, the bitumen viscosities decrease by one order of magnitude, indicating that the organic solvents have a good viscosity reducing effect.

3.2 Effect of SARA components

To study the individual roles of the SARA components in reducing the bitumen viscosity, saturate, aromatic, resin and asphaltene-toluene solutions were prepared. Fig. 5 shows the viscosities for concentrations in the range of 0–0.5 mg L^{-1} at 20 °C, and at a shear rate of 20 s^{-1}. For saturate, aromatic, resin, and asphaltene components, the SARA-toluene viscosity increases with the concentration of the SARA components. For the same concentration of the SARA components, the viscosity values were in the following order: saturate < aromatic < resin < asphaltene. As the saturate, aromatic, resin, and asphaltene components have different polarity and density, their influence on the bitumen viscosity is different. Although the asphaltene content in the toluene solution was low, asphaltene precipitants increase the viscosity, and asphaltene agglomerates increase with increasing asphaltene concentration.[12,41–43] This is consistent with the results obtained by Hemmati-Sarapardeh *et al.*[44]

3.3 Effects of SARA composite concentrations on viscosities of SARA-toluene solutions

Fig. 6 shows the effect of SARA composite concentrations on the viscosities of the SARA-toluene solutions.

The saturate/aromatic, saturate/resin, saturate/asphaltene, aromatic/resin, aromatic/asphaltene, and resin/asphaltene solutions were mixed and diluted in toluene with different concentrations. As shown in Fig. 6(a), when the concentration is in the range of 0.1–0.5 mg L^{-1}, the viscosity of the saturate/aromatic component is higher than that of the saturate component but lower than that of the aromatic component. The same is true for the saturate/resin (Fig. 6(b)) and saturate/asphaltene (Fig. 6(c)) components. However, Fig. 6(d)–(f) show that the viscosities of the mixed aromatic, resin, and asphaltene components are higher than those of the individual components at the same concentration. For example, the synergistic effect between the aromatic, resin, and asphaltene components in increasing the bitumen viscosity is obvious. This could be because all the aromatic, resin, and asphaltene components are aromatic organic compounds, and their mixture would aid resin and asphaltene aggregation. The more the aggregation, the higher the viscosity.

3.4 Effect of temperature on viscosities of 0.5 g mL^{-1} SARA-toluene solutions

The influence of temperature on the viscosities of the SARA-toluene solutions was studied, as shown in Fig. 7. Saturate-toluene, aromatic-toluene, resin-toluene, and asphaltene-toluene solutions at a concentration of 0.5 mg L^{-1} were used. The viscosity decreases with the increase in the temperature from 20 to 60 °C. The degree of viscosity reduction of the different solutions with temperature is as follows: asphaltene > resin > aromatic > saturate. This is because asphaltene and resin do not aggregate as much at higher temperatures.

3.5 Effect of temperature on bitumen viscosity under different nanoparticle concentrations

Fig. 8 shows the bitumen viscosity measurements in the presence of TiO_2 and CuO nanoparticles at concentrations of 0, 100, 500, 1000, 2500, and 10 000 mg L^{-1}, in the temperature range of 20–60 °C, and at a shear rate of 20 s^{-1}. The results show that the viscosity tends to decrease with the increase in the concentration of the nanoparticles in the bitumen. The can be mainly attributed to the absorption of the heavy components of bitumen by the nanoparticles, particularly asphaltene, and the consequent decrease in the aggregation of asphaltene.[45–47] With the increase in the nanoparticle concentration, the amount of asphaltene adsorbed increases, and the bitumen viscosity decreases. However, for the TiO_2 nanoparticles, the optimal concentration is 2500 mg L^{-1}

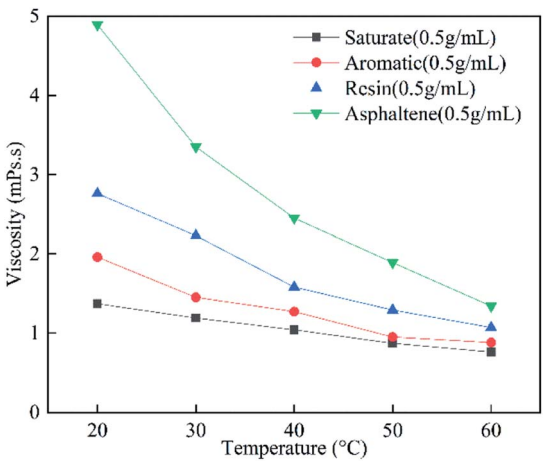

Fig. 7 Viscosities of saturate, aromatic, resin, and asphaltene-toluene solutions (0.5 g mL^{-1}) with different temperatures and at a shear rate of 20 s^{-1}.

 This journal is © The Royal Society of Chemistry 2020

Open Access Article. Published on 11 March 2020. Downloaded on 12/26/2025 7:02:38 PM.
This article is licensed under a Creative Commons Attribution-NonCommercial 3.0 Unported Licence.

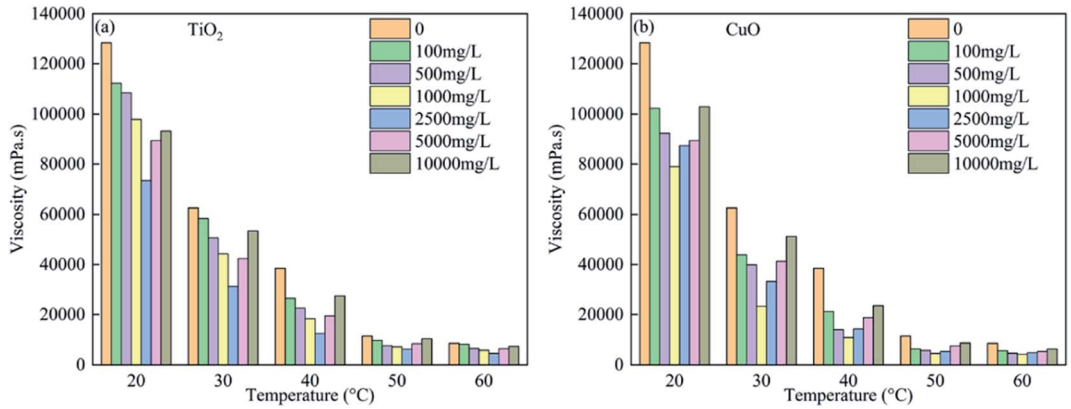

Fig. 8 Viscosity of bitumen in the presence of (a) TiO_2 nanoparticles; (b) CuO nanoparticles at different concentrations and temperatures ranging from 20 to 50 °C and at a shear rate of 20 s^{-1}.

(Fig. 8(a)). The optimal concentration of the CuO nanoparticles is 1000 mg L^{-1}. When the nanoparticle concentration is higher than the optimal concentration, the bitumen viscosity increases. This is because at higher nanoparticle concentrations, the packing factor of the particles increases, and the nanoparticles can aggregate. The interaction between the nanoparticles and the bitumen particles decreases, and a greater number of nanoparticles aggregate, thus increasing the bitumen viscosity.

For the TiO_2 and CuO nanoparticles, the bitumen viscosity decreases with increasing temperature. The reason for this is as follows. First, at higher temperatures, the viscosity of bitumen subfractions decreases, as shown in Fig. 8. Second, a greater amount of asphaltene is absorbed by the nanoparticles at higher temperatures.[48]

3.6 Effect of shear rate on bitumen viscosity under different nanoparticle sizes

Fig. 9 shows the variation in the bitumen viscosity in the presence of 2500 mg L^{-1} of TiO_2 nanoparticles and 1000 mg L^{-1} of CuO nanoparticles and with different sizes at 20 °C and a shear rate range of 20–80 s^{-1}. The viscosity reduction effect decreases with the increase in the nanoparticle size. For larger nanoparticles, the specific surface area decreases, and their ability to adsorb asphaltene becomes less. For a fixed size and concentration, the bitumen viscosity decreases with increasing shear rate.

3.7 Effect of ethyl cellulose concentration on bitumen viscosity

Fig. 10 shows the bitumen viscosity measurements in the presence of different concentrations of ethyl cellulose (Fig. 11(a)) and QASHI (Fig. 11(b)) at a temperature of 20 °C and a shear rate of 20 s^{-1}.

The bitumen viscosity decreases with the increase in the ethyl cellulose concentration. The synergistic effect between the aromatic, resin, and asphaltene components in increasing the bitumen viscosity is obvious, as shown in Fig. 11(a). Ethyl cellulose breaks the synergistic effect and decreases the viscosity between the aromatic, resin, and asphaltene components. For example, ethyl cellulose can break the resin or

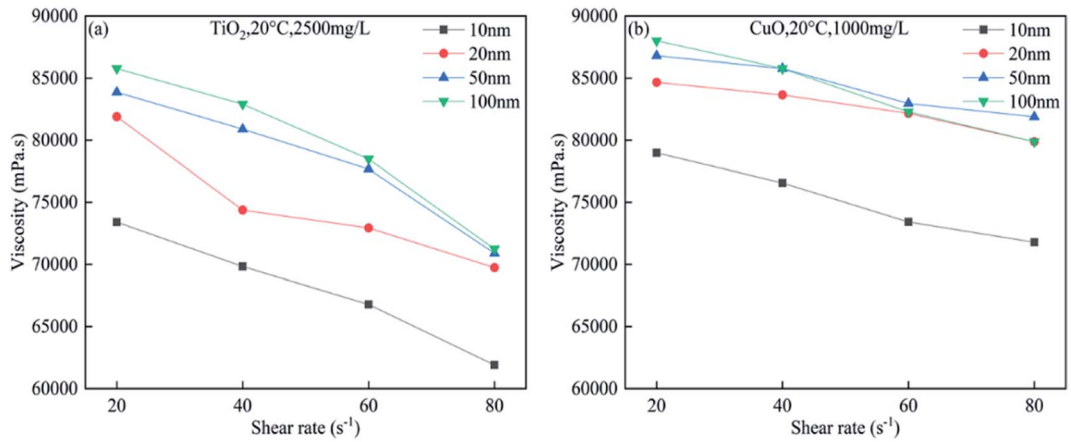

Fig. 9 Bitumen viscosity in the presence of (a) 2500 mg L^{-1} of TiO_2 nanoparticles; (b) 1000 mg L^{-1} of CuO nanoparticles of different sizes at 20 °C and a shear rate range of 20–80 s^{-1}.

Open Access Article. Published on 11 March 2020. Downloaded on 12/26/2025 7:02:38 PM.
This article is licensed under a Creative Commons Attribution-NonCommercial 3.0 Unported Licence.

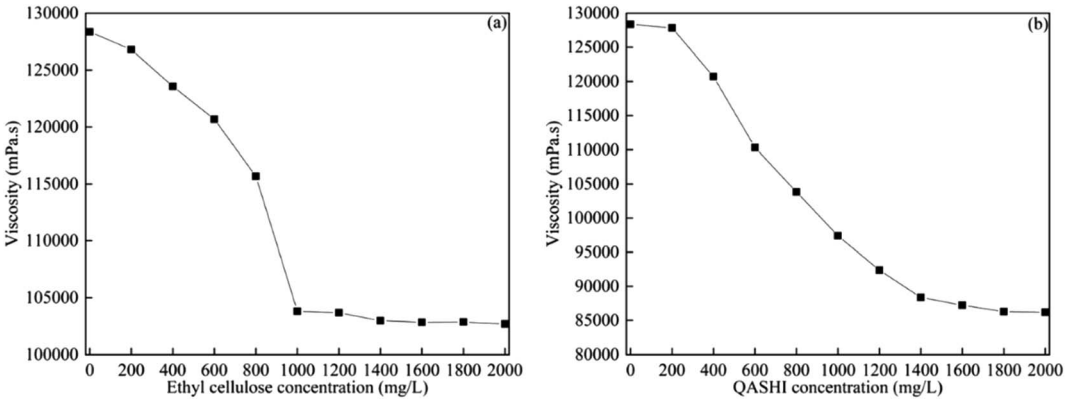

Fig. 10 Bitumen viscosity with different concentrations of (a) ethyl cellulose; (b) QASHI at 20 °C and at a shear rate of 20 s^{-1}.

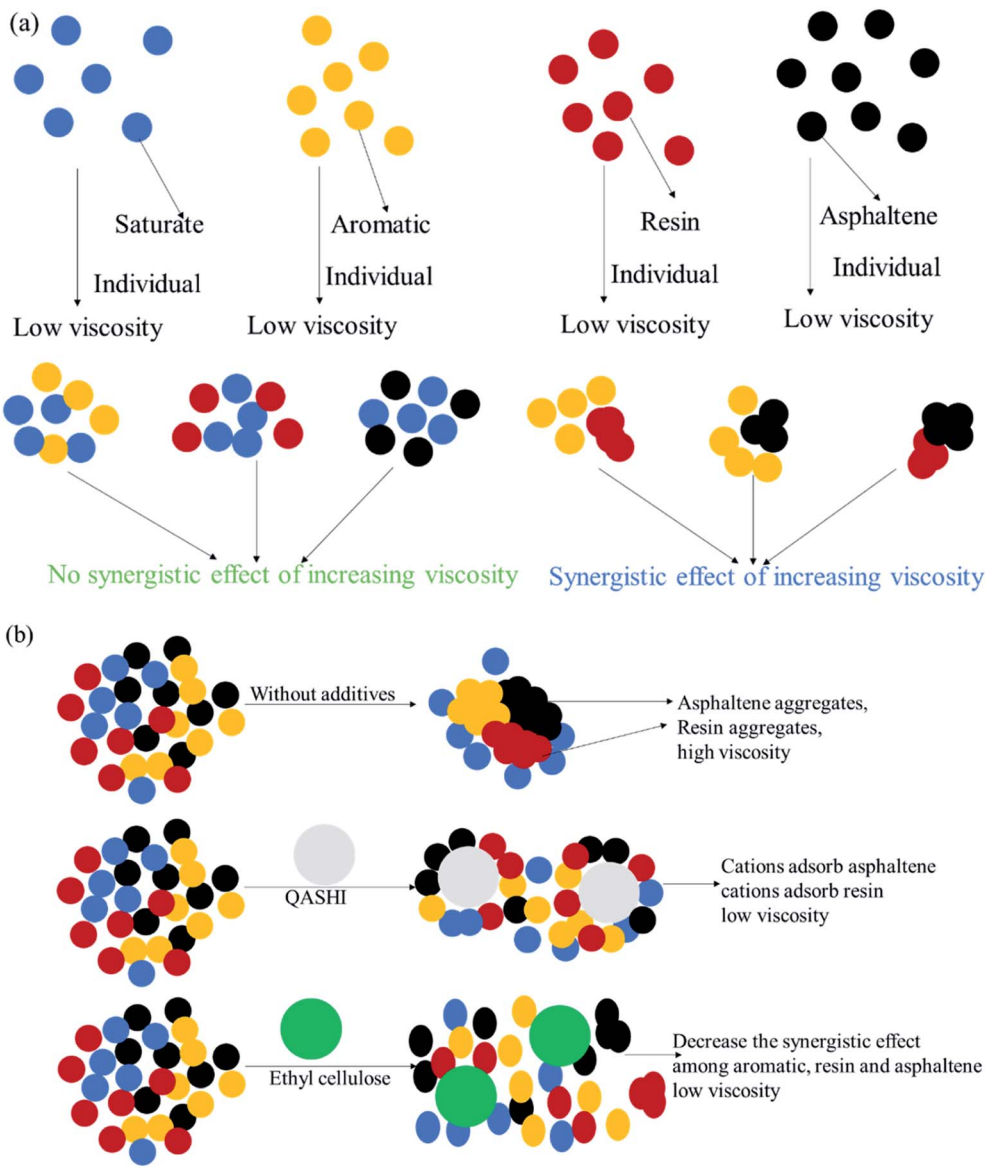

Fig. 11 (a) Synergistic effect of aromatic, resin, and asphaltene components on increasing viscosity; (b) mechanisms whereby ethyl cellulose and QASHI help decrease in bitumen viscosity.

This journal is © The Royal Society of Chemistry 2020

Open Access Article. Published on 11 March 2020. Downloaded on 12/26/2025 7:02:38 PM. This article is licensed under a Creative Commons Attribution-NonCommercial 3.0 Unported Licence.

asphaltene aggregates, as shown in Fig. 11(a). When the concentration of ethyl cellulose is higher than 1000 mg L^{-1}, the viscosity remains stable, because ethyl cellulose effectively breaks the resin and asphaltene aggregates, and more ethyl cellulose is redundant. The bitumen viscosity decreases with increasing QASHI concentration. The mechanism here is that QASHI could adsorb asphaltene because of the electrostatic interaction and work as cations, and as asphaltene is negatively charged, the asphaltenes were absorbed to a greater extent, thus decreasing the number of asphaltene aggregates, as shown in Fig. 11(b). However, when the QASHI concentration is higher than 1600 mg L^{-1}, the bitumen viscosity remains stable.

3.8 Synergistic effect of ethyl cellulose and nanoparticles on decreasing bitumen viscosity

Fig. 12 shows the synergistic effect of the nanoparticles with ethyl cellulose and QASHI in decreasing the bitumen viscosity. Ethyl cellulose along with the TiO_2 nanoparticles helps decrease the bitumen viscosity from 103 802 to 34 892 mPa s, which is lower than 73 402 mPa s (TiO_2). The decrease in the viscosity when ethyl cellulose was mixed with CuO nanoparticles is from 103 802 to 37 823 mPa s. The bitumen viscosity in the case of ethyl cellulose and nanoparticles is lower than that in the case of ethyl cellulose or nanoparticles individually. The reasons are as follows. Ethyl cellulose helps the nanoparticles to adsorb asphaltene, thus decreasing the number of asphaltene aggregates. Moreover, the nanoparticles work together with ethyl cellulose to destroy the synergistic effect of the aromatic, resin, and asphaltene components. QASHI along with TiO_2 nanoparticles could decrease the bitumen viscosity from 128 356 to 26 930 mPa s, which is much lower than 87 234 mPa s (QASHI only) and 73 402 mPa s (TiO_2 nanoparticles only). The synergistic effect between QASHI and CuO nanoparticles is also obvious. This can be attributed to the fact that QASHI and nanoparticles have a synergistic effect in increasing the asphaltene adsorption.

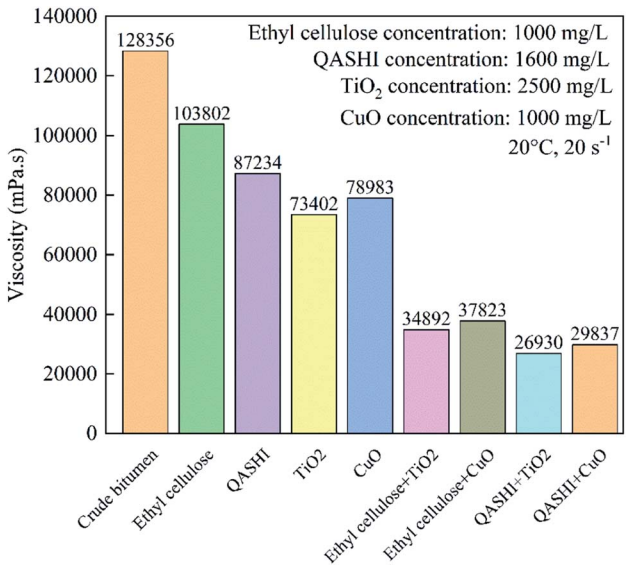

Fig. 12 Synergistic effect of nanoparticles with ethyl cellulose and QASHI in decreasing the bitumen viscosity at 20 °C and at a shear rate of 20 s^{-1}.

4. Conclusions

The highly viscous bitumen formed during the drilling of oilfields can significantly affect the drilling efficiency. To effectively remove bitumen, the reason for its high viscosity was studied, and the effect of SARA components on the bitumen viscosity was explored. Novel methods, including the use of organic solvents, TiO_2 nanoparticles, CuO nanoparticles, ethyl cellulose, and QASHI, were employed to decrease the viscosity of bitumen. The following conclusions can be drawn from this study:

(1) The organic solvent toluene exhibited the best effect in decreasing the bitumen viscosity, followed by *p*-xylene and cyclopentane. Under the same concentration, the viscosity values were as follows: saturate < aromatic < resin < asphaltene. The viscosity of the SARA-toluene solution increased with increasing SARA concentration. The aromatic, resin, and asphaltene components had a synergistic effect in increasing the viscosity. The viscosity decreased at elevated temperatures.

(2) TiO_2 and CuO nanoparticles were used to decrease the bitumen viscosity. The optimal concentrations of the TiO_2 and CuO nanoparticles were 2500 and 1000 mg L^{-1}, respectively. The viscosity of bitumen decreased with increasing nanoparticle concentration and then decreased. Below the optimal concentration, the bitumen viscosity decreased with increasing nanoparticle concentration, because the nanoparticles adsorbed resins and asphaltene to a greater extent. However, the bitumen viscosity increased with increasing nanoparticle concentration. For TiO_2 and CuO, at the same concentration, the bitumen viscosity decreased with increasing temperature. The viscosity reduction effect decreased with increasing nanoparticle size and increasing shear rate.

(3) The viscosity decreased with increasing ethyl cellulose and QASHI concentrations. Ethyl cellulose could break the resin and asphaltene aggregates and decrease the viscosity of bitumen. QASHI could adsorb asphaltene owing to electrostatic interaction and decrease the number of asphaltene aggregates. The optimal concentrations of ethyl cellulose and QASHI were 1000 and 1600 mg L^{-1}, respectively. The nanoparticles, ethyl cellulose, and QASHI could effectively reduce the viscosity of bitumen with a synergistic effect.

Abbreviations

QASHI: Quaternary ammonium salt of heptadecenyl hydroxyethyl imidazoline

Authors' contributions

Conceptualisation—LY, QZ; methodology—LY, ZH; validation—NZ, ZX; investigation—LY, ZC; data curation—LS, XX; writing—LY, ZH; funding acquisition—CZ, LS.

Open Access Article. Published on 11 March 2020. Downloaded on 12/26/2025 7:02:38 PM. This article is licensed under a Creative Commons Attribution-NonCommercial 3.0 Unported Licence.

Conflicts of interest

The authors declare no conflict of interests.

Acknowledgements

This work was financially supported by the 13th Five-Year Plan National Key Project of China (No. 2017ZX05005005-006), the National Major Science and Technology Project of China (No. 2017ZX05032-004-005, No. 2017ZX05030-001), the National Natural Science Foundation of China (No. 51974354 and No. 51704322) and the CNOOC Project (No. 2019KJ-ZC02).

References

1 H. Chen, S. Zhang, Z. Zhao, M. Liu and Q. Zhang, Application of dopamine functional materials in water pollution control, *Prog. Chem.*, 2019, **31**, 571–579.

2 M. Meng, Z. Qiu, R. Zhong, Z. Liu, Y. Liu and P. Chen, Adsorption characteristics of supercritical CO_2/CH_4 on different types of coal and a machine learning approach, *Chem. Eng. J.*, 2019, **368**, 847–864.

3 L. Ping, X. Wang and K. Zou, The application of cluster drilling technology in high pressure salt gypsum formation in swamp wetland of NA oilfield of Iran. *IADC/SPE Asia Pacific Drilling Technology Conference*, Society of Petroleum Engineers, Singapore, 2016.

4 Y. H. Zhang, X. M. Xu, M. Lebedev, M. Sarmadivaleh, A. Barifcani and S. Iglauer, Multi-scale x-ray computed tomography analysis of coal microstructure and permeability changes as a function of effective stress, *Int. J. Coal Geol.*, 2016, **165**, 149–156.

5 S. Rudyk, Relationships between SARA fractions of conventional oil, heavy oil, natural bitumen and residues, *Fuel*, 2018, **216**, 330–340.

6 L. Carbognani, L. C. Roa-Fuentes, L. Diaz, F. Lopez-Linares, A. Vasquez, P. Pereira-Almao, P. Haghigat, B. B. Maini and R. J. Spencer, *Pet. Sci. Technol.*, 2010, **28**, 632–645.

7 X. G. Li, J. J. Hou, H. Sui, L. Y. Sun and L. Xu, Switchable-Hydrophilicity Triethylamine: Formation and Synergistic Effects of Asphaltenes in Stabilizing Emulsions Droplets, *Materials*, 2018, **11**, 10.

8 F. Nie, D. M. He, J. Guan, X. Q. Li, Y. Hong, L. F. Wang, H. A. Zheng and Q. M. Zhang, Oil sand pyrolysis: Evolution of volatiles and contributions from mineral, bitumen, maltene, and SARA fractions, *Fuel*, 2018, **224**, 726–739.

9 J. H. Hao, Y. J. Che, Y. Y. Tian, D. W. Li, J. H. Zhang and Y. Y. Qiao, Thermal cracking characteristics and kinetics of oil sand bitumen and its SARA fractions by TG-FTIR, *Energy Fuels*, 2017, **31**, 1295–1309.

10 C. A. Franco, M. M. Lozano, S. Acevedo, N. N. Nassar and F. B. Cortés, Effects of resin I on asphaltene adsorption onto nanoparticles: A novel method for obtaining asphaltenes/resin isotherms, *Fuel*, 2016, **30**, 264–272.

11 L. Padula, L. B. D. S. Balestrin, N. D. O. Rocha, H. W. Jr, M. B. Cardoso, E. Sabadini and W. J. E. Loh, Role of asphaltenes and additives on the viscosity and microscopic structure of heavy crude oils, *Fuel*, 2016, **30**, 3644–3651.

12 X. Li, Y. Guo, S. Qiang, W. Lan and X. Guo, Effect of nanoparticles on asphaltene aggregation in a microsized pore, *Ind. Eng. Chem. Res.*, 2018, **57**, 9009–9017.

13 S. W. Hasan, M. T. Ghannam and N. J. F. Esmail, Heavy crude oil viscosity reduction and rheology for pipeline transportation, *Fuel*, 2010, **89**, 1095–1100.

14 J. G. Lu, S. J. Chen, X. L. Wang, Y. Wang, J. Z. Zhang and Z. H. Shi, Characteristics and origin analysis of viscous oil and reservoir bitumen in Santai-Beisantai area, *J. China Univ. Pet., Ed. Nat. Sci.*, 2011, **35**, 27–31.

15 P. B. Manesh, K. Shahbazi and S. Shahryari, Application of grid partitioning based fuzzy inference system and ANFIS as novel approach for modeling of Athabasca bitumen and tetradecane mixture viscosity, *Pet. Sci. Technol.*, 2019, **37**, 1613–1619.

16 A. K. Mehrotra, Development of mixing rules for predicting the viscosity of bitumen and its fractions blended with toluene, *Can. J. Chem. Eng.*, 2010, **68**, 839–848.

17 T. Ning, Z. Deng, J. G. Dai, K. Yang, C. Chen and Q. Wang, Geopolymer as an additive of warm mix asphalt: Preparation and properties, *J. Cleaner Prod.*, 2018, **192**, 906–915.

18 R. Pal, A new model for the viscosity of asphaltene solutions, *Can. J. Chem. Eng.*, 2015, **93**, 747–755.

19 E. J. Suarez-Dominguez, A. Palacio-Perez, A. Rodriguez-Valdes, S. Gonzalez-Santana and E. Izquierdo-Kulich, Effect of a viscosity reducer on liquid-liquid flow: III. Partial mixing on the interface, *Pet. Sci. Technol.*, 2017, **36**, 79–84.

20 R. N. Traxler and C. U. Pittman, Penetration-viscosity relationship for asphaltic bitumen, *J. Appl. Phys.*, 1937, **8**, 70–71.

21 W. B. W. Nik, F. N. Ani, H. H. Masjuki and S. G. E. Giap, Rheology of bio-edible oils according to several rheological models and its potential as hydraulic fluid, *Ind. Crops Prod.*, 2005, **22**, 249–255.

22 S. Mortazavi-Manesh and J. M. Shaw, Effect of diluents on the rheological properties of Maya crude oil, *Energy Fuels*, 2016, **30**, 766–772.

23 A. Y. Malkin, G. Rodionova, S. Simon, S. O. Ilyin, M. P. Arinina, V. G. Kulichikhin and J. Sjoblom, Some compositional viscosity correlations for crude oils from Russia and Norway, *Energy Fuels*, 2016, **30**, 9322–9328.

24 R. Hashemi, N. N. Nassar and P. P. Almao, Enhanced heavy oil recovery by *in situ* prepared ultradispersed multimetallic nanoparticles: A study of hot fluid flooding for Athabasca bitumen recovery, *Energy Fuels*, 2013, **27**, 2194–2201.

25 M. T. Ghannam, S. W. Hasan, B. Abu-Jdayil and N. Esmail, Rheological properties of heavy & light crude oil mixtures for improving flowability, *J. Pet. Sci. Eng.*, 2012, **81**, 122–128.

26 I. Raj, M. Qu, L. Z. Xiao, J. R. Hou, Y. F. Li, T. Liang, T. Y. Yang and M. D. Zhao, Ultralow concentration of molybdenum disulfide nanosheets for enhanced oil recovery, *Fuel*, 2019, **251**, 514–522.

27 T. Wijayanto, M. Kurihara, T. Kurniawan and O. Muraza, Experimental investigation of aluminosilicate

 This journal is © The Royal Society of Chemistry 2020

Open Access Article. Published on 11 March 2020. Downloaded on 12/26/2025 7:02:38 PM.
This article is licensed under a Creative Commons Attribution-NonCommercial 3.0 Unported Licence.

nanoparticles for enhanced recovery of waxy crude oil, *Energy Fuels*, 2019, **33**, 6076–6082.

28 A. Bila, J. A. Stensen and O. Torsaeter, Experimental investigation of polymer-coated silica nanoparticles for enhanced oil recovery, *Nanomaterials*, 2019, **9**, 25.

29 Y. Kazemzadeh, S. Shojaei, M. Riazi and M. Sharifi, Review on application of nanoparticles for EOR purposes: A critical review of the opportunities and challenges, *Chin. J. Chem. Eng.*, 2019, **27**, 237–246.

30 A. S. Dalkilic, O. A. Turk, H. Mercan, S. Nakkaew and S. Wongwises, *Int. Commun. Heat Mass Transfer*, 2019, **107**, 1–13.

31 M. M. Sarafraz, B. Yang, O. Pourmehran, M. Arjomandi and R. Ghomashchi, Fluid and heat transfer characteristics of aqueous graphene nanoplatelet (GNP) nanofluid in a microchannel, *Int. Commun. Heat Mass Transfer*, 2019, **107**, 24–33.

32 X. Li, J. Hou, H. Sui, L. Sun and L. Xu, Switchable-hydrophilicity triethylamine: Formation and synergistic effects of asphaltenes in stabilizing emulsions droplets, *Mater*, 2018, **11**, 2431.

33 Y. Liu, Z. Qiu, H. Zhong, Z. Nie, J. Li, W. Huang and X. Zhao, Bitumen recovery from crude bitumen samples from H Oilfield by single and composite solvents—Process, parameters, and mechanism, *Mater*, 2019, **12**, 2656.

34 X. H. Feng, S. Q. Wang, J. Hou, L. X. Wang, C. Cepuch, J. Masliyah and Z. H. Xu, Effect of Hydroxyl Content and Molecular Weight of Biodegradable Ethylcellulose on Demulsification of Water-in-Diluted Bitumen Emulsions, *Ind. Eng. Chem. Res.*, 2011, **50**, 6347–6354.

35 X. H. Feng, Z. H. Xu and J. Masliyah, Biodegradable Polymer for Demulsification of Water-in-Bitumen Emulsions, *Energy Fuels*, 2009, **23**, 451–456.

36 E. Pensini, D. Harbottle, F. Yang, P. Tchoukov, Z. F. Li, I. Kailey, J. Behles, J. Masliyah and Z. H. Xu, Demulsification Mechanism of Asphaltene-Stabilized Water-in-Oil Emulsions by a Polymeric Ethylene Oxide–Propylene Oxide Demulsifier, *Energy Fuels*, 2014, **28**, 6760–6771.

37 L. He, F. Lin, X. G. Li, Z. H. Xu and H. Sui, Enhancing heavy oil liberation from solid surfaces using biodegradable demulsifiers, *J. Environ. Chem. Eng.*, 2016, **4**, 1753–1758.

38 J. Hou, X. H. Feng, J. Masliyah and Z. H. Xu, Understanding Interfacial Behavior of Ethylcellulose at the Water-Diluted Bitumen Interface, *Energy Fuels*, 2012, **26**, 1740–1745.

39 T. Wang, C. Zhang, R. Y. Zhao, C. J. Zhu, C. H. Yang and C. G. Liu, Solvent extraction of bitumen from oil sands, *Energy Fuels*, 2014, **28**, 2297–2304.

40 K. Pal, N. Branco, A. Heintz, P. Choi, Q. Liu, P. R. Seidl and M. R. Gray, Performance of solvent mixtures for non-aqueous extraction of Alberta oil sands, *Energy Fuels*, 2015, **29**, 2261–2267.

41 R. Aminzadeh, M. Nikazar and B. Dabir, The effect of nonylphenol on asphaltene aggregation: A molecular dynamics approach, *Pet. Sci. Technol.*, 2019, **37**, 1883–1890.

42 N. J. H. Dunn, B. Gutama and W. G. Noid, Simple simulation model for exploring the effects of solvent and structure on asphaltene aggregation, *J. Phys. Chem. B*, 2019, **123**, 6111–6122.

43 R. Aminzadeh, M. Nikazar and B. Dabir, Determining the occurrence time of different stages of asphaltene aggregation using molecular dynamics simulations, *Pet. Sci. Technol.*, 2019, **37**, 2101–2107.

44 A. Hemmati-Sarapardeh, B. Dabir, M. Ahmadi, A. H. Mohammadi and M. M. Husein, Toward mechanistic understanding of asphaltene aggregation behaviour in toluene: The roles of asphaltene structure, aging time, temperature, and ultrasonic radiation, *J. Mol. Liq.*, 2018, **264**, 410–424.

45 A. Varamesh and N. Hosseinpour, Prediction of asphaltene precipitation in reservoir model oils in the presence of Fe_3O_4 and NiO nanoparticles by cubic plus association equation of state, *Ind. Eng. Chem. Res.*, 2019, **58**, 4293–4302.

46 X. Li, Y. Guo, Q. Sun, W. Lan, A. Liu and X. Guo, Experimental study for the impacts of flow rate and concentration of asphaltene precipitant on dynamic asphaltene deposition in microcapillary medium, *J. Pet. Sci. Eng.*, 2018, **162**, 333–340.

47 M. Igder, N. Hosseinpour, A. A. Biyouki and A. Bahramian, Control of asphaltene aggregation in reservoir model oils along the production streamline by Fe_3O_4 and NiO nanoparticles, *Energy Fuels*, 2018, **32**, 6689–6697.

48 J. Castillo, V. Vargas, V. Piscitelli, L. Ordoñez and H. Rojas, Study of asphaltene adsorption onto raw surfaces and iron nanoparticles by AFM force spectroscopy, *J. Pet. Sci. Eng.*, 2017, **151**, 248–253.